Anal. Chem. **2002,** *74,* 5342−5349

Measuring the Number of Independent Emitters in Single-Molecule Fluorescence Images and Trajectories Using Coincident Photons

Kenneth D. Weston,† Martina Dyck, Philip Tinnefeld, Christian Müller, Dirk P. Herten, and Markus Sauer*

Physikalisch-Chemisches Institut, Universität Heidelberg, Im Neuenheimer Feld 253, 69120 Heidelberg, Germany

A simple new approach is described and demonstrated for measuring the number of independent emitters along with the fluorescence intensity, lifetime, and emission wavelength for trajectories and images of single molecules and multichromophoric systems using a single PC plug-in card for time-correlated single-photon counting. The number of independent emitters present in the detection volume can be determined using the interphoton times in a manner similar to classical antibunching experiments. In contrast to traditional coincidence analysis based on pulsed laser excitation and direct measurement of coincident photon pairs using a time-to-amplitude converter, the interphoton distances are retrieved afterward by recording the absolute arrival time of each photon with nanosecond time resolution on two spectrally separated detectors. Intensity changes that result from fluctuations of a photophysical parameter can be distinguished from fluctuations due to changes in the number of emitters (e.g., photobleaching) in single chromophore and multichromophore intensity trajectories. This is the first report to demonstrate imaging with contrast based on the number of independently emitting species within the detection volume.

In recent years, several innovations in fluorescence imaging and spectroscopy techniques have made possible, and in fact routine, the detection and study of individual molecules at room temperature.[1−3] Single-molecule studies allow one to observe fluctuations in the fluorescent properties of individual molecules over time (dynamic disorder) as well as variations in fluorescent properties of chemically identical molecules located in different environments within the same heterogeneous sample (static disorder). Some phenomena that would not necessarily be predicted based on knowledge of ensemble measurements but are readily observed by looking at single molecules include fluctuations in fluorescence intensity,[4−6] fluorescence lifetime,[5−7] triplet lifetime,[8,9] wavelength,[10−12] and dipole orientation.[13−17] The ability to distinguish between one and multiple molecules is extremely important as single-molecule studies are progressively having more impact on the current understanding of molecular dynamics and photophysics. There are numerous examples of multichromophoric systems that are currently being intensely researched using fluorescence imaging and trajectory analysis. These include both molecules produced by nature such as the red fluorescent protein DsRed,[18−20] allophycocyanine,[7] B-phycoerythrin, and the light-harvesting complex LH2[5,21] and synthetic light-emitting molecules such as poly(*p*-phenylene−vinylene) (PPV),[22] poly(*p*-pyridylene−vinylene),[22] and MEH−PPV[23] and various chromophoric dendrimers.[24−26] In addition, a number of

* To whom correspondence should be addressed. E-mail: sauer@urz.uni-heidelberg.de. Phone: +49-6221-548460. Fax: +49-6221-544255.

† Present address: Department of Chemistry and Biochemistry, Florida State University, Tallahassee, FL 32306.

(1) Nie, S. M.; Chiu, D. T.; Zare, R. N. *Science* **1994**, *266*, 1018−1021.
(2) Betzig, E.; Chichester, R. J. *Science* **1993**, *262*, 1422−1425.
(3) Macklin, J. J.; Trautman, J. K.; Harris, T. D.; Brus, L. E. *Science* **1996**, *272*, 255−258.
(4) Weston, K. D.; Carson, P. J.; Metiu, H.; Buratto, S. K. *J. Chem. Phys.* **1998**, *109*, 7474−7485.
(5) Bopp, M. A.; Jia, Y. W.; Li, L. Q.; Cogdell, R. J.; Hochstrasser, R. M. *Proc. Natl. Acad. Sci. U.S.A.* **1997**, *94*, 10630−10635.
(6) Tinnefeld, P.; Buschmann, V.; Herten, D. P.; Han, K.-T.; Sauer, M. *Single Mol.* **2000**, *1*, 215−223.
(7) Ying, L. M.; Xie, X. S. *J. Phys. Chem. B* **1998**, *102*, 10399−10409.
(8) Weston, K. D.; Carson, P. J.; DeAro, J. A.; Buratto, S. K. *Chem. Phys. Lett.* **1999**, *308*, 58−64.
(9) Veerman, J. A.; Garcia-Parajo, M. F.; Kuipers, L.; van Hulst, N. F. *Phys. Rev. Lett.* **1999**, *83*, 2155−2158.
(10) Lu, H. P.; Xie, X. S. *Nature* **1997**, *385*, 143−146.
(11) Ha, T.; Enderle, T.; Chemla, D. S.; Selvin, P. R.; Weiss, S. *Chem. Phys. Lett.* **1997**, *271*, 1−5.
(12) Tinnefeld, P.; Herten, D. P.; Sauer, M. *J. Phys. Chem. A* **2001**, *105*, 7989−8003.
(13) Ruiter, A. G. T.; Veerman, J. A.; GarciaParajo, M. F.; vanHulst, N. F. *J. Phys. Chem. A* **1997**, *101*, 7318−7323.
(14) Ha, T.; Enderle, T.; Chemla, D. S.; Selvin, P. R.; Weiss, S. *Phys. Rev. Lett.* **1996**, *77*, 3982.
(15) Ha, T.; Glass, J.; Enderle, T.; Chemla, D. S.; Weiss, S. *Phys. Rev. Lett.* **1998**, *80*, 2093−2096.
(16) Weston, K. D.; Goldner, L. S. *J. Phys. Chem. B* **2001**, *105*, 3453−3462.
(17) Deschenes, L. A.; Vanden Bout, D. A. *Science* **2001**, *292*, 255−258.
(18) Garcia-Parajo, M. F.; Koopman, M.; van Dijk, E.; Subramaniam, V.; van Hulst, N. F. *Proc. Natl. Acad. Sci. U.S.A.* **2001**, *98*, 14392−14397.
(19) Cotlet, M.; Hofkens, J.; Habuchi, S.; Dirix, G.; Van Guyse, M.; Michiels, J.; Vanderleyden, J.; De Schryver, F. C. *Proc. Natl. Acad. Sci. U.S.A.* **2001**, *98*, 14398−14403.
(20) Lounis, B.; Deich, J.; Rosell, F. I.; Boxer, S. G.; Moerner, W. E. *J. Phys. Chem. B* **2001**, *105*, 5048−5054.
(21) Bopp, M. A.; Sytnik, A.; Howard, T. D.; Cogdell, R. J.; Hochstrasser, R. M. *Proc. Natl. Acad. Sci. U.S.A.* **1999**, *96*, 11271−11276.
(22) VandenBout, D. A.; Yip, W. T.; Hu, D. H.; Fu, D. K.; Swager, T. M.; Barbara, P. F. *Science* **1997**, *277*, 1074−1077.
(23) Hu, D. H.; Yu, J.; Barbara, P. F. *J. Am. Chem. Soc.* **1999**, *121*, 6936−6937.
(24) Hofkens, J.; Maus, M.; Gensch, T.; Vosch, T.; Cotlet, M.; Kohn, F.; Herrmann, A.; Mullen, K.; De Schryver, F. *J. Am. Chem. Soc.* **2000**, *122*, 9278−9288.

10.1021/ac025730z CCC: $22.00
Published on Web 09/10/2002

biological processes occur on the level of a few molecules, for example, enzymes in biomolecular machines such as transcription factories or replication foci.[27,28] The ability to determine the number of molecules present in a small detection volume could be useful for identifying interacting, colocalized, molecules that cannot be resolved optically.

In single-molecule studies, several characteristics have frequently been assumed to confirm that the fluorescence observed is in fact derived from only a single emitter. For example, whereas it is known that in ensemble measurements photobleaching results in a decay of the fluorescence intensity over time, one expects a single molecule to photobleach in a single, instantaneous step. The observation of transient dark states, i.e., when the fluorescence intensity reversibly drops to the background despite continuous illumination, has also been assumed to be an indication that the signal is from a single molecule, as multiple emitters would not be expected to go into these dark states simultaneously. Two other proofs are tested using the polarization properties of excitation and emission light. Single dye molecules are expected to have a well-defined absorption and emission dipole orientation; to lack this unique property would mean that multiple, nonparallel emitters generate the detected fluorescence.[13−17]

Another property of a single emitter that differs from that of a cluster or ensemble is that the probability of emitting two consecutive photons drops to zero for time intervals shorter than the excited-state lifetime. In simple terms, the molecule cannot emit two photons simultaneously. After photon emission, a molecule must be re-excited and wait, on average, one fluorescence lifetime before another photon can be emitted. This property of the photon arrival time statistics, termed photon antibunching, has been measured at room temperature under continuous wave illumination by averaging over a number of molecules [29] as well as pulsed laser illumination for individual molecules.[30,31] For both cases, the typical measurement uses the Hanbury-Brown and Twiss setup:[32] the fluorescence emission is split and detected on two single-photon avalanche diodes (SPADs). A time-to-amplitude converter measures the time intervals between photons (one detector channel is the start, and the other the stop). These are ordered in a histogramm to get the interphoton arrival times distribution. For pulsed laser excitation, as we use it, the distribution of arrival times is largely dominated by the laser repetition rate, as interphoton times are always a multiple of the interval between laser pulses (neglecting background counts, which arrive at random, and the uncertainty due to the excited-state S_1 lifetime). For a single emitter, the zero peak, which represents pairs of fluorescence photons generated during a single laser pulse, is necessarily vacant as long as the laser pulse width is much shorter than the molecule's fluorescence lifetime (again neglecting background). This technique represents one of very few realized methods for distinguishing between a single emitter and an aggregate or cluster.

The investigation of multichromophore systems such as light-emitting polymers, chromophoric dendrimers, photonic wires, and biological complexes will also obviously benefit from the application and development of tools capable of determining the number of emitters present. Single-molecule studies of these systems have exhibited interesting quantum effects. For example, as expected in cases in which internal energy transfer occurs, a species with multiple absorbing moieties may result in only a single emitting species.[22,24] Therefore, intermittent fluorescence and discrete emission levels might be observed. Efficient energy-hopping processes might even give rise to the observation of photon antibunching in multichromophore systems.[33] However, in most systems, it is still not clear how many chromophores contribute to the measured fluorescence signal. Only through careful study of these systems can we hope to elucidate an understanding of their photophysics.

Dynamic fluctuations in the properties of the fluorescence from single chromophores can reveal a wealth of information regarding the molecular motions of the molecule itself and the environment in which it resides,[10] as well as the nonradiative energy-transfer processes between the fluorophore and other chemical species in close proximity.[24] It is advantageous to monitor multiple parameters (e.g., intensity, spectrum, lifetime, orientation) to more accurately characterize the dynamics observed. In a recent paper, we demonstrated the ability to monitor single-molecule antibunching in time.[30] In that report, three separate PC plug-in boards were used: one collected spectral and intensity information, another was used for time-correlated single-photon counting (TCSPC) to monitor the fluorescence lifetime, and a third board (also a TCSPC) was used to measure interphoton times.[30] Since then, we have developed new methods that make these measurements far more practical and easy and we have synchronized the acquisition with sample scanning so that the measurements can be performed in imaging mode. The new instrument can perform the measurements using a single PC plug-in TCSPC board (see Figure 1). In addition, we have produced samples of a Cy5-DNA-Cy5 construct to obtain colocalized fluorophores for the purpose of testing and demonstrating the method. The new method also has higher efficiency in terms of photon collection for antibunching measurements, which is extremely important for this technique to work effectively.

The TCSPC board we use records for each photon (a) the arrival time after the beginning of the acquisition with a resolution of 50 ns and (b) the time delay between the start pulse (fluorescence) and stop pulse (laser) with a time resolution of 6 ps (although this is limited to ∼200 ps by jitter on the detector electronic signal). These will be referred to as the macroscopic time and the microscopic time, respectively. In addition, the TCSPC board records the channel (SPAD 1 or SPAD 2) from which each photon was detected. Because the TCSPC card has a dead time of 125 ns, it is necessary to apply an electronic delay

(25) Gensch, T.; Hofkens, J.; Heirmann, A.; Tsuda, K.; Verheijen, W.; Vosch, T.; Christ, T.; Basche, T.; Mullen, K.; De Schryver, F. C. *Angew. Chem., Int. Ed.* **1999**, *38*, 3752−3756.

(26) Vosch, T.; Hofkens, J.; Cotlet, M.; Kohn, F.; Fujiwara, H.; Gronheid, R.; Van Der Biest, K.; Weil, T.; Herrmann, A.; Mullen, K.; Mukamel, S.; Van der Auweraer, M.; De Schryver, F. C. *Angew. Chem., Int. Ed.* **2001**, *40*, 4643−+.

(27) Pombo, A.; Jackson, D. A.; Hollinshead, M.; Wang, Z. X.; Roeder, R. G.; Cook, P. R. *EMBO J.* **1999**, *18*, 2241−2253.

(28) Leonhardt, H.; Rahn, H. P.; Cardoso, M. C. *J. Cell. Biochem.* **1998**, *243*, 3-+.

(29) Ambrose, W. P.; Goodwin, P. M.; Enderlein, J.; Semin, D. J.; Martin, J. C.; Keller, R. A. *Chem. Phys. Lett.* **1997**, *269*, 365−370.

(30) Tinnefeld, P.; Müller, C.; Sauer, M. *Chem. Phy Lett.* **2001**, *343*, 252−258.

(31) Lounis, B.; Moerner, W. E. *Nature* **2000**, *407*, 491−493.

(32) Hanbury-Brown, R.; Twiss, R. Q. *Nature* **1956**, *177*, 27.

(33) Wu, M.; Goodwin, P. M.; Ambrose, W. P.; Keller, R. A. *J. Phys. Chem.* **1996**, *100*, 17406−17409.

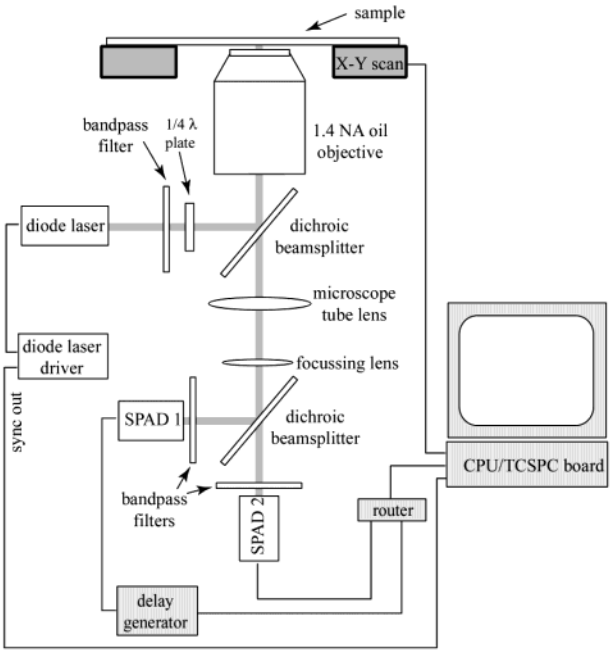

Figure 1. Diagram of the experimental setup. Fluorescence induced by a pulsed diode laser is split nearly 50:50 into short-λ and long-λ emission channels and detected at two avalanche photodiodes. The channel, macroscopic arrival time, and microscopic arrival time are recorded for each photon using a time-correlated single-photon counting PC plug-in board.

to one of the two SPAD signals such that two fluorescence photons generated by the same laser pulse can both be detected. Treatment of the data to obtain the appropriate signature of antibunching is simplified when the time interval between laser pulses is the same as or longer than the macroscopic time resolution of 50 ns. In the demonstration provided here, we use a laser that pulses every 100 ns (repetition rate, 10 MHz), exactly twice that of the macroscopic time resolution of our TCSPC board. The experimental arrangement and data analysis described in this report is a convenient way to monitor the fluorescence intensity, lifetime, and spectral position of fluorescing species while simultaneously measuring the number of independent emitters during the trajectories.

MATERIALS AND METHODS

The dye Cy5 (Amersham Life Science Inc.) was obtained as functionalized *N*-hydroxysuccinimidyl ester. The following 40-mer complementary oligonucleotides, (**i**) 5′- ***A**TA TAA GCT ATG CAA TGC TAT GGT AAC GTA TCG AAT CGT A-3′ and (**ii**) 5′-T ACG A**T***T CGA TAC GTT ACC ATA GCA TTG CAT AGC TTA TAT-3′, were custom-synthesized by Carl Roth GmbH (Karlsruhe, Germany). One Cy5 was coupled to the 5′-end of oligonucleotide **i** via 5′-amino modifier C_6 and the other was coupled to C_6 amino-modified thymidine bases in the complementary oligonucleotide **ii** resulting in a Cy5/Cy5 distance of 35 base pairs. The coupling reactions were carried out in 250 mM carbonate buffer, pH 9.3, at room temperature for 2 h. The labeled oligonucleotides were purified by reversed-phase (RP18 column) HPLC (Beckman Instruments Inc., Fullerton, CA) using a gradient of 0−75% acetonitrile in 0.1 M aqueous triethylammonium acetate. Complementary labeled oligonucleotides were mixed 1:1 at room temperature in 100 mM Tris borate, pH 8.3, containing 1 M NaCl. For imaging, the DNA constructs were adsorbed on standard cover slides with a thickness of 170 μm and dried under nitrogen prior to use. A treatment with 10^{-10} M solutions of the DNA constructs yielded an area density of less than 1 molecule/μm^2.

A fiber-coupled, pulsed 635-nm laser diode (10-MHz repetition rate, pulse width <100 ps, average excitation power 4 kW/cm^2; Picoquant, Berlin, Germany) and two spectrally separated detectors were employed in a sample scanning confocal microscope to image and monitor the fluorescence from single molecules immobilized on glass coverslips. The collimated laser beam is sent through a band-pass filter and a quarter-wave retarder oriented to ensure circularly polarized light and then directed into the back port of an inverted microscope. Within the microscope, the laser beam was reflected by a dichroic mirror and focused to a tight spot by an oil-immersion objective (100×, NA = 1.4). Fluorescence collected by the same objective was split by a dichroic mirror at ~670 nm and focused onto the active areas of two SPADs of the same type.

The sample *x* and *y* positions were controlled using a closed-loop piezostage with a parallel PC interface for imaging the sample and positioning individual fluorescing spots in the focused excitation beam. An automated search routine operates as follows. The sample is scanned across a 20-μm line (the *x* axis). In the event that a signal above a threshold count rate of 50 kHz is observed, the stage returns to the line position of maximum intensity and records the fluorescence continuously until the molecule is photobleached. The *y*-axis position is stepped by 300 nm and the process is repeated.

The signal from one of the two SPADs was delayed using a delay generator (Stanford Research DG535). Both signals were fed into the router of a TCSPC PC interface board (SPC-630; Becker & Hickl, Berlin, Germany), and the laser sync signal (10 MHz) was connected to the board's sync input. In this arrangement, both of the SPAD signals can operate as the "start" signal of the time-to-amplitude converter (TAC) and the laser sync operates as the "stop" signal. Time-resolved data are acquired using the FIFO mode in which the microscopic arrival time, the macroscopic arrival time, and the detection channel (SPAD 1 or SPAD 2) is registered for each fluorescence photon detected.

The electronic delay was applied to the signal from the SPAD detecting the shorter wavelength fluorescence and was set at 948 ns. Any delay time longer than the TCSPC dead time can be used. We selected this particular delay time because, in combination with the cable lengths we used and the settings of the TCSPC card (for example, the constant fraction discriminator levels, time-to-amplitude gain and offset, etc.), this delay time places the resulting fluorescence lifetime decays from both SPAD channels at the same position in our 25-ns TAC window. In addition, the 948-ns time delay was selected so that photons generated by the same laser pulse appeared at 20 macroscopic resolution time units apart (see Figure 2b). The ratio of fluorescence intensity detected at the SPADs is proportional to the peak emission wavelength and allows us to monitor spectral fluctuations. Note that the dependence is not linear but is useful nonetheless and can be corrected to be quantitative to some extent.[12] For efficient determination of fluorescence lifetimes, we

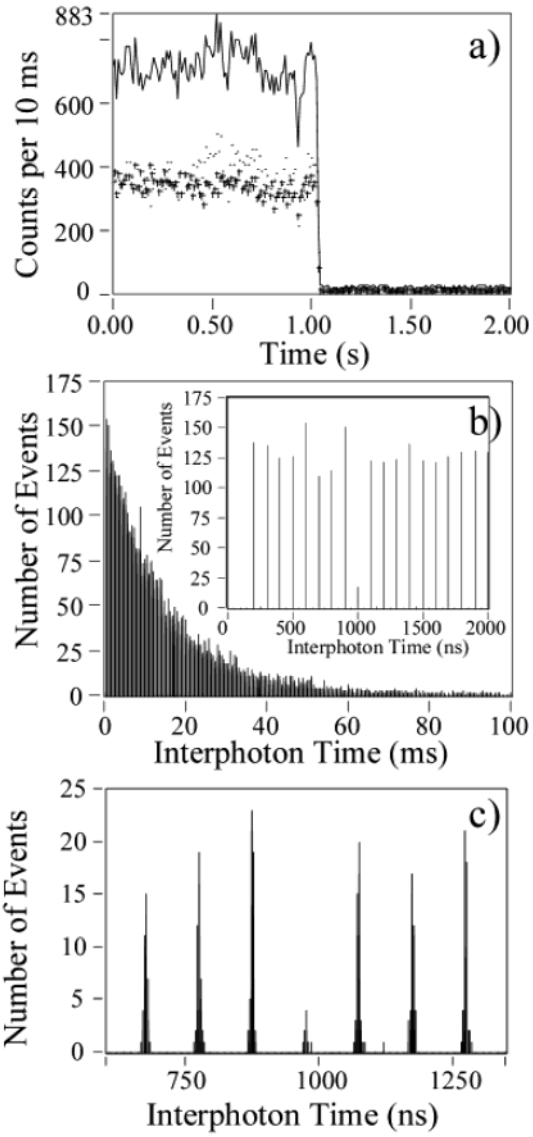

Figure 2. Fluorescence trajectory and coincidence data for a Cy5-DNA construct with one Cy5 molecule. The total fluorescence intensity as a function of time is shown in (a). The distribution of interphoton times obtained from the macroscopic arrival times is shown in (b). The inset shows the same data in the time range around the zero peak, which corresponds to photon pairs that were induced by the same laser pulse. In (c), both the macroscopic and microscopic arrival times are combined before calculating the interphoton times and creating the distribution. The $N_C/\bar{N}_L$ ratio for these data is 0.14 ± 0.03.

applied a maximum likelihood estimator (MLE) algorithm.[34] Thus, the fluorescence intensity, emission maximum (fractional intensity, $F_2 = I_2/[I_1 + I_2]$), and lifetime are monitored simultaneously. In addition, the macroscopic arrival times are used to calculate the interphoton times. When the macroscopic time of a long-λ photon is detected and followed by a short-λ photon, and the separation time is 20 macroscopic resolution units (the same as our added electronic delay), this is a coincident event, and we know that the two photons were induced by the same laser pulse. The ratio of the number of these coincident photon events to the number of noncoincident photon pairs (i.e., interphoton times in peaks neighboring the zero peak, dubbed "lateral peaks"; see Figure 2b) for a given time interval gives a measure of the number of independently emitting fluorophores.[30,31,35] In the ideal case, this ratio is 0 for a single emitter and 1 for an ensemble of molecules and falls between 0 and 1 for several independent emitters.

RESULTS AND DISCUSSION

As mentioned previously, interphoton times were obtained with the use of the macroscopic times (by simply subtracting the macroscopic time of the preceding photon for each photon). Because the time between laser pulses is 100 ns and the macroscopic time resolution is 50 ns, there is one laser pulse every other macroscopic time bin. A histogram of the interphoton times therefore has peaks spaced 100 ns apart, or one peak for every two macroscopic resolution units.

Note that it is possible, although unnecessary for our purposes, to combine the macroscopic time and microscopic time to obtain the absolute arrival time with picosecond resolution. However, it is worth pointing out that the SPC-630 TCSPC plug-in board actually records the macroscopic time of the laser sync signal that follows the fluorescence photon, which may not always be the same as the arrival time of the fluorescence photon. In our case, the laser sync signal that follows the detection of a fluorescence photon will always be a little less than 100 ns (100 ns less the lifetime of the excited state). As a result, all of the recorded macroscopic times are shifted (incorrect) by two macroscopic resolution units (~100 ns). However, since our analysis uses the interphoton times, subtraction of any macroscopic time from the macroscopic time of the previous photon removes the constant 100-ns shift and it has no impact on the final results.

Since the electronic 948-ns delay was applied to the signal from the short-λ SPAD, we know that two detected photons induced by the same laser pulse will always be detected as a long-λ channel photon followed by a short-λ channel photon (with interphoton time near 948 ns). Since we also record the channel from which each photon was detected, we can select only those interphoton times that are appropriate (long-λ followed by short-λ). Only these interphoton times are included in interphoton arrival times distributions. For events for which two fluorescence photons are induced by the same laser pulse but are directed toward the same SPAD, a coincidence event will not be recognized because two photons cannot both be detected simultaneously at a single SPAD. The frequency of detecting these events (first a long-λ channel photon and then a short-λ channel photon) is highest when the total count rate from each SPAD is equal, so it is important to have the fluorescence signal split as evenly as possible between the two detectors. It is also important that the relative contribution of fluorescence signal detected from each molecule in the detection volume is the same. Thus, we use circularly polarized light for the best possible excitation of all chromophores even if their absorption dipole orientations are distributed randomly. Nevertheless, we do see variations in the emitted intensity due to molecules with absorption dipoles that are aligned partially along the *z* axis or have variable emission yield due to differences in conformation or local environment.

(34) Tellinghuisen, J.; Goodwin, P. M.; Ambrose, W. P.; Martin, J. C.; Keller, R. A. *Anal. Chem.* **1994**, *66*, 64.

(35) Brunel, C.; Lounis, B.; Tamarat, P.; Orrit, M. *Phys. Rev. Lett.* **1999**, *83*, 2722−2725.

To demonstrate the methods described, images and fluorescence trajectories were acquired from a sample of DNA constructs consisting of two Cy5 fluorophores separated by 35 base pairs dispersed on a glass coverslip with a surface density appropriate for single-molecule studies. For these DNA constructs, the Cy5 chromophores are separated by a distance of ~12 nm (assuming 0.34 nm/base) and no chromophore interaction via dipole−dipole interactions is expected. Although we should in principle have two Cy5 dyes colocalized at every DNA strand adsorbed to the surface, fluorescence trajectories indicative of single Cy5 chromophores were sometimes observed (~30%). This might be due to denaturation of the 40-mer double-strand upon adsorption on the glass surface or to very fast photobleaching of one of the two Cy5 chromophores before we are able to detect it. An example trajectory of a single Cy5 dye is shown in Figure 2a. The detected count rate of 65 kHz was split nearly equally between the two detectors and persisted for just over 1 s before a single-step photobleach. Figure 2b shows the distribution of interphoton times between 0 and 100 μs for short-λ photons followed by long-λ photons detected prior to the photobleaching event. The inset in Figure 2b shows an expanded view of the same data between 0 and 2 μs. There are several relevant features to mention from this figure. The most important of these is the lower number of events in the peak at 1000 μs, which corresponds to the number of photon pairs induced by the same laser pulse. For a single emitter with a fluorescence lifetime that is long compared to the laser pulse, we would expect no zero-time photon pairs. There are two reasons why there are zero-time photon pairs. The first is a result of the nonzero background. Accidental coincidences due to background−background, signal−background, and background−signal contributions can generate photon pairs in the zero peak. The second possibility is due to the finite laser pulse width (~100 ps). There is a very small but nonzero probability that a molecule could go through one excitation−emission cycle in a short time interval and then be re-excited by the energy in the tail of the same laser pulse. The data in these histograms can be quantified for the purpose of determining the number of independent emitters by determining the ratio of the number of photons in the central peak, N_C, to the average number in the neighboring lateral peaks, $\bar{N}_L$. As illustrated in Figure 2b, the number of counts in the neighboring peaks decreases at large interphoton times but is nearly constant for very short times (e.g., 0−2 μs). For $\bar{N}_L$, we use the average number of events in the nearest 16 peaks, 8 to each side of the zero-time peak. For this single Cy5 molecule, the ratio $N_C/\bar{N}_L$ is 0.14 ± 0.03. All of the trajectories of single Cy5 molecules we have measured give a ratio in the range 0.05−0.2, depending on the F_2, background, and signal levels (See eq 4 and corresponding discussion below). Another feature to note in Figure 2b is the fact that no events are recorded for delay times of 100 ns; these photon pairs cannot be detected due to the dead time of the SPC board.

Figure 2c shows the distribution of the interphoton times for the same data, but for which the macroscopic and microscopic arrival times for each photon were combined to calculate the absolute arrival times prior to calculating the interphoton times. This step is not necessary for our purposes but is demonstrated here because this type of plot is typical of what is normally measured using the Hanbury-Brown and Twiss setup in which a TAC is used to record interphoton times. Note that the measurement method we demonstrate here is fundamentally different from those reported previously because it does not rely on a time-to-amplitude converter for measuring the interphoton times. Instead, the arrival time of each photon is recorded and the interphoton times are tabulated afterward. For measuring the number of independent emitters, the TAC is not necessary. It is only used for determining the fluorescence lifetime decays.

Figure 3a shows the total intensity trajectory (from both SPADS) of a double-labeled DNA construct. Multiple intensity levels are observed including an off level (signal = background), which is a common characteristic of the Cy5 dye on dry glass surfaces.[6,12] Panels b and c of Figure 3 show the fractional intensity, F_2, and fluorescence lifetime, τ_f, respectively, each calculated with 10-ms resolution. Fluctuations in the F_2 value and τ_f are observed as in the previous studies. Since discrete intensity fluctuations are known to occur for single Cy5 molecules, it would be pure speculation to declare that the large intensity drop at 1.0 s is due to the photobleaching of one of the two Cy5 fluorophores. The coincidence method, however, lets us answer this question definitively. To determine the number of emitting species with time using the coincidence method, we selected only photon pairs that generated interphoton times in the central peak and plotted the number of these events during each 100 ms of the trajectory. (Figure 3d). The rate of occurrence of these central peak photons drops from ~4/100 ms to nearly zero after 1.0 s, indicating the photobleaching of the first of the two Cy5 chromophores. To quantify the number of fluorophores emitting before and after this initial photobleaching event, Figure 3e shows the ratio $N_C/\bar{N}_L$ during the trajectory. The ratio $N_C/\bar{N}_L$ drops substantially after 1.0 s. The distributions of interphoton times taken from the period before and after the photobleaching event (indicated by an arrow in Figure 3a) are shown in panels g and h in Figure 3, respectively. The ratio $N_C/\bar{N}_L$ drops from 0.39 ± 0.06 for the photons collected prior to 1.0 s to 0.14 ± 0.04 for the photons detected after 1.0 s. A ratio of 0.5 is expected for two molecules detected with equal intensity.[30] The ratio $N_C/\bar{N}_L$ will deviate from this ideal case if, as in our case, the two fluorophores are not detected with equal intensity. From the intensity trajectory in Figure 3a, we can see that ~70% of the total count rate can be attributed to the Cy5 that bleached first, so we expect a deviation from the expected ratio of 0.5. Nevertheless, based on the large change in the measured ratio before and after 1.0 s, we can definitively assign the large intensity drop to a photobleaching event. An expression that can be used to predict and better understand the deviation of the measured $N_C/\bar{N}_L$ ratio from that expected for the ideal case for any given case is derived and presented below.

The fluorescence lifetime decays obtained from the measured microscopic times of the photons detected before and after 1.0 s are plotted separately in Figure 3f to show clearly the jump in fluorescence lifetime that occurred. Between 0 and 1.0 s, the fluorescence lifetime of the two-dye complex was 2.5 ns, and after 1.0 s, it was 3.4 ns. Note that the data are collected in the reverse time mode and the x axis of the histogram corresponds to the actual measured microscopic arrival times.

As with the trajectories, the coincidence events can be selected, counted, and analyzed to reveal new information about the number of independently emitting molecules in an image format. Figure

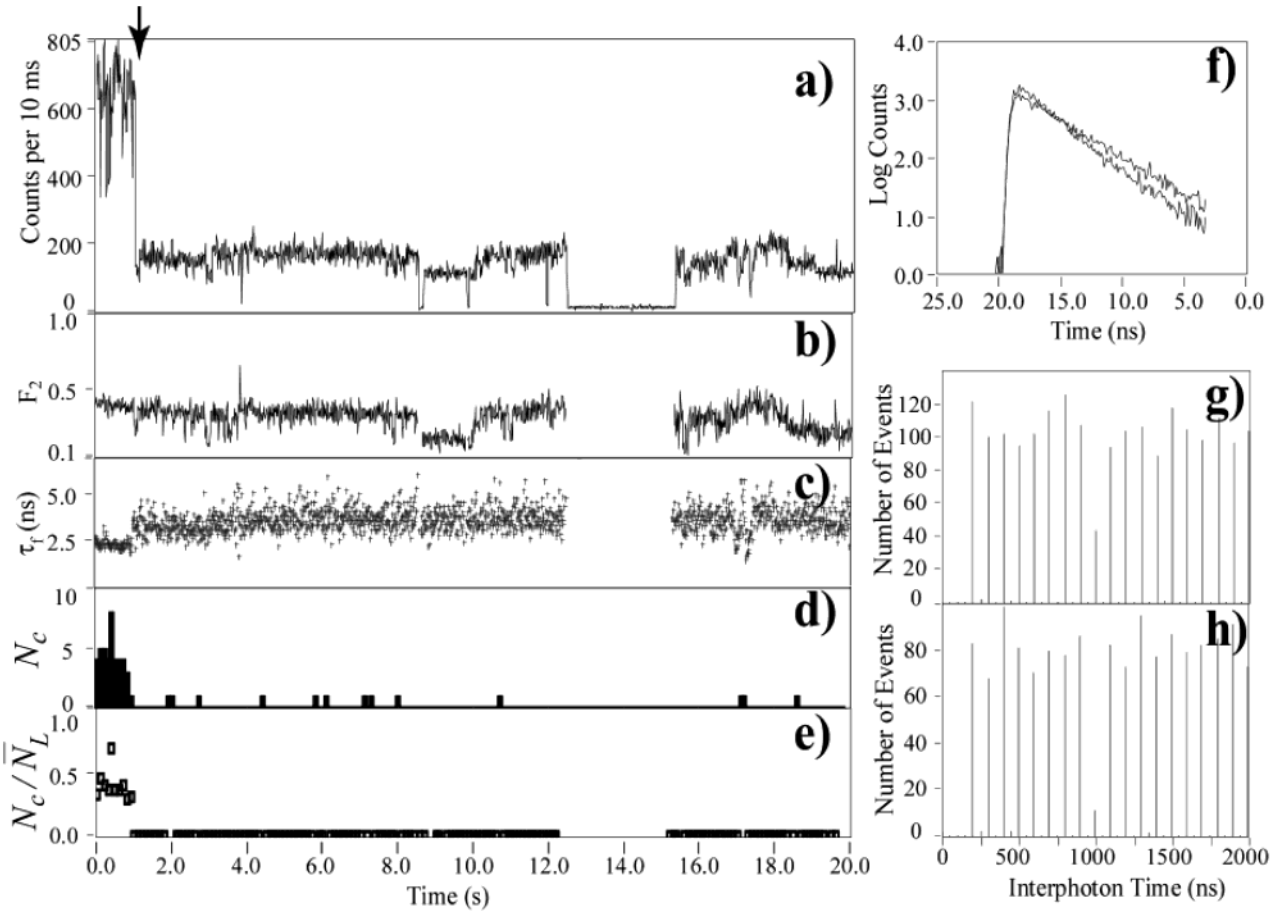

Figure 3. Multiparameter trajectories and selected data measured for a Cy5-DNA-Cy5 construct. The total intensity (a), fractional intensity, F_2 (b), fluorescence lifetime, τ_f (c), number of zero-peak coincidence counts, N_C (d), and $N_C/\bar{N}_L$ ratio (e) are shown as a function of time. The distributions of interphoton times for photons measured before and after the time indicated by the arrow in (a) are shown in (g) and (h), respectively. The $N_C/\bar{N}_L$ ratio in (g) is 0.39 ± 0.06 and in (h) it is 0.14 ± 0.04, indicating that the large drop in intensity can be attributed to the photobleach of the first of two Cy5 molecules that were emitting at the beginning of the trace. The distributions of microscopic arrival times, i.e., the fluorescence decays, are shown in (f) for the photons collected before and after the photobleach.

4a shows the total intensity image of a sample of the double-labeled DNA construct. The integration time per pixel is 15 ms, and the excitation power is 4 μW. Figure 4b shows the corresponding image if we use only the zero-peak photons. The gray scale in this image runs from zero to four coincidence events. A single line trace through this image is analogous to the trajectory in Figure 3d. For selected regions of the image where the brightest spots are observed (indicated by the dashed squares) we can analyze the data to obtain the distribution of interphoton times and $N_C/\bar{N}_L$ ratios the same way as described for a trajectory. Integrating the N_C and N_L values for all the pixels within the dashed squares, we calculated the ratios $N_C/\bar{N}_L$ of 0.49 ± 0.09 for the spot labeled (1), and 0.16 ± 0.06 for the spot labeled (2). From these results, we can attribute spot 1 to two independently emitting Cy5 molecules while spot 2 can be assigned to a single Cy5 molecule.

An expression for the ratio of the number of counts in the coincidence peak, N_C, to the average number of counts in the neighboring lateral peaks, $\bar{N}_L$, is derived in the following section. We assume n independently emitting molecules are in the confocal detection volume and consider all possible ways that a central peak photon pair might be generated. The indexes i and j are used to represent molecules 1 ... n. During any single laser pulse, two fluorescence photons can be detected when molecules i and j both emit, except for the case $i = j$, which represents a single molecule emitting two photons during the laser pulse. We can also account for the fact that the F_2 value and the detected fluorescence count rate from each molecule is not necessarily the same. The probability that a photon is emitted by molecule i is p_i, where the total fluorescence count rate is normalized so that $\sum_i p_i = 1$. The product $(F_2)_i p_i$ is the probability that a photon from molecule i is detected at SPAD 2 and the product $(1 - F_2)_j p_j$ is the probability that a photon from molecule i is detected at SPAD 1. Hence, $(F_2)_i(1 - F_2)_j p_i p_j$ is the probability that both events occur. For all possible combinations of these probabilities for the n molecules, we obtain the probability of detecting a photon pair induced by the same laser pulse, f_C:

$$f_C = \sum_{i=1}^{n} \sum_{j=1, j\neq i}^{n} (F_2)_i(1 - (F_2)_j)p_i p_j \qquad (1)$$

The same expression as in eq 1 can be used to calculate the probability of detecting pairs of consecutively detected photons

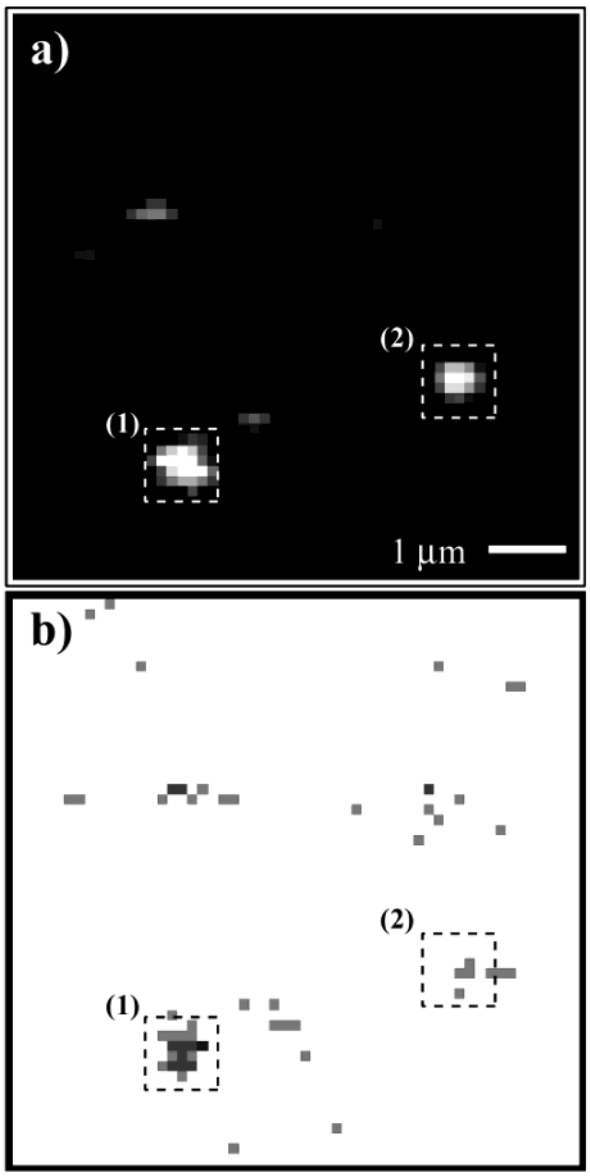

Figure 4. Total fluorescence intensity image (a) and the corresponding zero-peak image (b). The bright spot (1) has an $N_C/\bar{N}_L$ ratio of 0.49 ± 0.09, and spot (2) has an $N_C/\bar{N}_L$ ratio of 0.16 ± 0.06; therefore spot 1 can be attributed to two independently emitting Cy5 molecules while spot 2 can be assigned to a single Cy5 molecule. The integration time was 15 ms/pixel with pixel size of 133 nm.

that are noncoincident (i.e., interphoton times in the lateral peaks), with the restriction, $j \neq i$, removed:

$$f_L = \sum_{i=1}^{n}\sum_{j=1}^{n}(F_2)_i(1-(F_2)_j)p_i p_j \qquad (2)$$

The ratio $N_C/\bar{N}_L$ can then be calculated as simply

$$N_C/\bar{N}_L = f_C/f_L \qquad (3)$$

We can also account for the background at the two SPAD channels. Typically, the background of the short-λ channel is higher than the long-λ channel due to more leakage of the Rayleigh scatter through the filters in front of the short-λ channel SPAD. The background signal is denoted B_1 and B_2 at the short-λ and long-λ channels, respectively, and S is the total fluorescence signal level. Zero peak, coincident photon pairs, as well as neighboring, noncoincident photon pairs can be caused by background−background, background−signal, or signal−signal photon pairs. Thus, the following equation for the ratio $N_C/\bar{N}_L$ takes into account the background signal:

$$N_C/N_L = \frac{B_1B_2 + S\overline{F_2}B_2 + S\overline{(1-F_2)}B_1 + f_C S^2}{B_1B_2 + S\overline{F_2}B_2 + S\overline{(1-F_2)}B_1 + f_L S^2} \qquad (4)$$

where

$$\overline{F_2} = \sum_{i=1}^{n}(F_2)_i p_i \quad \text{and} \quad \overline{(1-F_2)} = \sum_{i=1}^{n}(1-(F_2)_i)p_i$$

The expected ratio $N_C/\bar{N}_L$ calculated using eq 4 is demonstrated for some specific cases in Figure 5. In Figure 5a, the expected ratio $N_C/\bar{N}_L$ is calculated for 1−10 independent emitters. The bottom curve is for the ideal case in which the background is zero, each emitter contributes equally to the total fluorescence signal (i.e., $p_i = 1/n$), and each molecule has $F_2 = 0.5$. This curve shows that the incremental change in $N_C/\bar{N}_L$ ratio decreases with the number of emitters; thus, the method will be most useful for measuring small numbers of emitters. It will be more difficult to accurately determine the number of independent emitters when higher numbers are present. The additional curves in Figure 5a show the calculation with the same ideal parameters but with background added equally in both channels. The S/B ratio for the curves above are 100:1, 20:1, 10:1, 5:1, and 2:1. As one would intuitively expect, the effect of adding background signal is to reduce the distinction between few and many emitters to give a ratio $N_C/\bar{N}_L$ closer to the ensemble value of 1. Figure 5b shows the expected ratio $N_C/\bar{N}_L$ as a function of S/B for one emitter (bottom curve), two emitters, and three emitters (top curve), again assuming that each molecule contributes equally to the total fluorescence signal and $F_2 = 0.5$ for all molecules. This curve shows that even with a high S/B of 100, we cannot expect an absolutely zero $N_C/\bar{N}_L$. This result substantiates the nonzero $N_C/\bar{N}_L$ ratio we measured for single Cy5 molecules, as in the data of Figure 2. Figure 5c shows the expected ratio $N_C/\bar{N}_L$ for two emitters (each with $F_2 = 0.5$, and a S/B of 30), demonstrating what happens to the ratio $N_C/\bar{N}_L$ when the two molecules are not detected equally (i.e., as a function of $p_1/p_1 + p_2$). When the total signal is almost exclusively from one or the other molecule, but not both, a ratio $N_C/\bar{N}_L$ close to zero is calculated, as for a single emitter.

The expression in eq 4 is extremely important for the coincidence technique not only for comparison of the experimental data with theoretical values but also for determining within a single-molecule trajectory whether an intensity jump was due to a photobleach or whether it was due to a change of photophysical properties.-Likewise, the expression can be used to evaluate the number of emitters in single molecule coincidence images.

Although rich in information, the fluorescence intensity, lifetime, and fractional intensity trajectories contain no direct

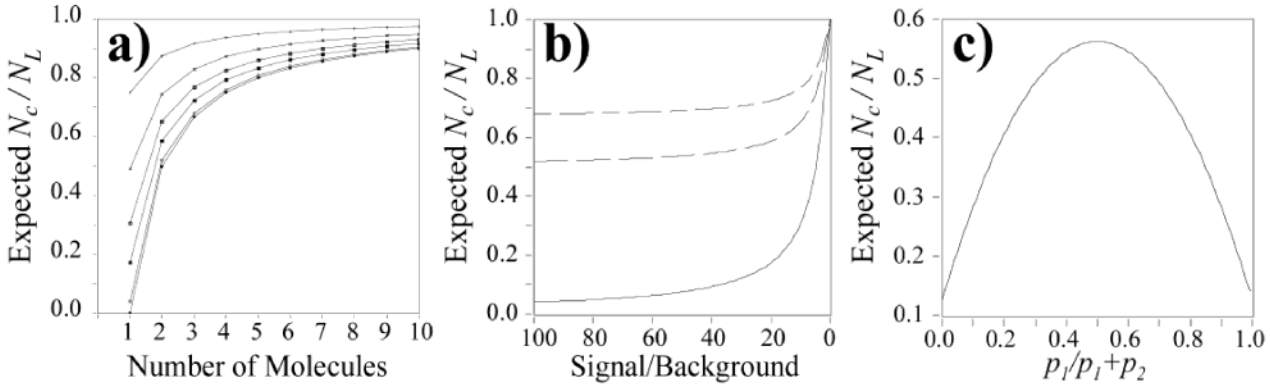

Figure 5. Expected ratio $N_C/\bar{N}_L$ calculated using eq 4 for some specific cases. In (a), the expected ratio $N_C/\bar{N}_L$ is calculated for 1−10 independent emitters for the ideal case in which $p_i = 1/n$; each molecule has an F_2 value of 0.5. In the bottom curve, the background is zero and the above curves have S/B ratios of 100:1, 20:1, 10:1, 5:1, and 2:1. In (b), the ratio $N_C/\bar{N}_L$ as a function of S/B for one emitter (bottom curve), two emitters, and three emitters (top curve) are shown. The plot in (c) shows the expected ratio $N_C/\bar{N}_L$ for two emitters (each with $F_2 = 0.5$, and a S/B of 30) demonstrating what happens to the ratio $N_C/\bar{N}_L$ when the two molecules are not detected equally.

information about the number of emitting chromophores. In addition, we cannot accurately assign the observed changes in fluorescence intensity, spectrum, or lifetime to an interchromophore interaction. The addition of the coincidence analysis is an easily implemented and an important advance for the accurate interpretation of single-molecule fluorescence trajectories and images.

CONCLUSIONS

We have demonstrated a simple and convenient technique for measuring interphoton separation times for the purpose of detecting antibunching in the fluorescence emitted from single, or very few, molecules. The described method uses a hardware setup similar to that commonly used in a number of laboratories around the world that measure fluorescence lifetime and multiparameter trajectories of single fluorescent molecules and multichromophoric systems. Therefore, the widespread implementation as a standard parameter for single-molecule investigations is inevitable. By measuring the number of independently emitting fluorophores in time and space, accurate interpretations of single-molecule trajectories and images will be facilitated. Besides applications in the investigation of multichromophoric entities, this technique, which is based on the quantum mechanical phenomenon of antibunching, might also be promising for applications in molecular biology.

ACKNOWLEDGMENT

This work was supported by the Volkswagen-Stiftung (Grant I/78 094) and the Bundesministerium für Bildung, Wissenschaft, Forschung und Technologie (Grants 311864/13N8352).

Received for review April 23, 2002. Accepted July 11, 2002.

AC025730Z